Chapter 3

Fabrication and Characterization of Pd/ZnO Thin Film Schottky Diodes Grown on n-Si Substrates

3.1. Introduction

It is observed from the discussions presented in Chapter 1 and Chapter 2 that the ZnO thin film based Schottky diodes have drawn considerable attention in recent times due to their possible applications as UV photodetectors [Liang *et al*. (2001), Soci *et al*. (2007)], gas sensors [Huang and Choi (2007), Kyoung and Jang (2010)], solar cells [Chopra *et al*. (2004)] and piezoelectric nanogenerators [Wang and Song (2006)] etc. It is also discussed in Chapter 2 that large work function based metals such as Pt (5.65), Pd (5.12) and Au (5.1) [Sze (1981), Lajn *et al*. (2009), Brillson and Lu (2011)] are normally preferred for achieving large barrier heights and small leakage currents of the ZnO thin film based Schottky contacts [Mead (1966), Sze (1981)]. However, Pd has drawn special interests of the researchers for fabricating the Schottky contacts on ZnO thin films grown by different techniques on different substrates including sapphire, GaAs, glass, Si etc [Weichsel *et al*. (2005), Wenckstern *et al*. (2006), Schifano *et al.* (2007)]. The present Chapter deals with the fabrication and characterization of Pd/ZnO thin film based Schottky diodes on n-Si substrates using thermal evaporation method. We have used an n-Si substrate due to its flexibility of integration with the CMOS circuits as well as possible ohmic nature of the n-Si/n-ZnO heterojunctions already discussed in Chapter-2. The outline of the present Chapter can be given as follows:

Section 3.2 presents the experimental details of the Pd/ZnO thin film Schottky contacts grown on n-Si <100> substrates by the thermal evaporation method. Section 3.3 includes the results and discussions related to ZnO film and Pd/ZnO Schottky diode characterizations. First, the results related to various structural and optical characterizations

of ZnO thin films by analyzing the FESEM image, EDS, XRD and PL spectrum have been discussed. Then, the room temperature capacitance-voltage (C-V) and temperature-dependent current–voltage (I-V) characteristics of the as-fabricated Pd/ZnO thin film Schottky diodes under consideration have been analyzed in this section. A Gaussian function for the random barrier height distribution at Pd/ZnO interface has been used for including the effects of barrier inhomogeneity phenomenon [Werner and Güttler (1991)] on various electrical parameters such as the barrier height, ideality factor and Richardson constant of the Schottky diodes. Finally, the summary and conclusion of this chapter have been presented in Section 3.4.

3.2. Experimental Details

In this section, we will discuss the details of the experimental procedure used for the fabrication of Pd/ZnO thin film based Schottky diodes grown on n-Si substrates by thermal evaporation method. The fabrication process includes the substrate cleaning, ZnO thin films deposition by thermal evaporation method on properly cleaned n-Si substrates, annealing of the films in N_2 gas atmosphere, deposition of Pd metal dots on ZnO thin films for Schottky contacts and deposition of Ti/Al on the entire back surface of the Si substrates for ohmic contact deposition under study. The above fabrication steps are discussed in details in the following sub-sections.

3.2.1 Substrates Cleaning

The ultra-sonication method was first used to clean the n-silicon (Si) <100> substrates (4$^{//}$) of resistivity ρ = 1-6 Ω cm (Wacker-Chemitronic GmbH, Germany) using trichloroethylene (TCE) for 15 minutes followed by dipping in acetone for 2 minutes. The n-Si substrates were then placed in the solution of H_2SO_4:H_2O_2 in the ratio of 40:60 to remove the organic contamination from the substrates surfaces by subsequent rinsing in de-ionized (DI) water (ρ = 18 MΩ-cm) of Milli-Q water plant of Millipore, USA. Finally, the substrates were dipped in the solution of HF: DI water in the ratio of (1:6) to remove the native oxide layer from the substrates surface. The as-mentioned process is well known as Piranha–HF Method. We have used this process of Si substrate cleaning for fabricating various devices presented in Chapter 3-6 of the present thesis.

3.2.2 ZnO Film Deposition by the Thermal Evaporation Method

The thermal evaporation is one of the most widely used techniques of physical vapor deposition (PVD) [Smith (1994), Özgür *et al.* (2005), Ali and Chakrabarti (2012)]. In this method, the source material is evaporated in a vacuum closed chamber and vacuum allows vapor particles to travel directly to the target object (substrate) where they condense back to a solid state as schematically represented in Fig. 3.1. The thermal evaporation mechanism thus includes two basic processes: the first process deals with the evaporation of material while the second process is the condensation of the evaporated material particles on the substrate's surface. The source materials to be evaporated are placed on the heated semimetal (ceramic) evaporators, known as "boats" due to their shape. The materials are first melted in the boat cavity due to heat and are then evaporated in a high vacuum environment into a cloud above the source. The substrate (i.e. target) on which the deposition has to be performed is placed at a certain distance from the source (i.e. boat). The evaporated particles can travel directly to the deposition target without colliding with the background gas in the high vacuum environment. It may be mentioned that hot objects (e.g. the heating filaments) in the evaporation chamber may produce unwanted vapors which can degrade the quality of the vacuum in the chamber to some extent [Smith (1994)]. The thickness of the as-deposited thin films of the desired material can be monitored by a quartz crystal micro-balance attached with the thermal evaporation unit.

In the present work, the n-Si substrates were placed immediately after cleaning in the thermal evaporation unit (model no. 12A4D of HINDVAC, India) with a base pressure of 10^{-3} mPa inside the chamber. The ultrapure ZnO powder (99.99%) purchased from the MERK-Chemical limited; Mumbai, India was used as the source material for ZnO deposition. The ZnO powder was converted into pellets of 10 mm diameter by using the hot pressure set up. The as-fabricated ZnO pellets were then placed on the molybdenum boat for evaporation by resistive heating in the evaporation unit at a deposition rate of 0.10 nm/s. The evaporation time was set at 55 min and the distance between the substrate and source was maintained at 18 cm. The desired ZnO film of ~300 nm thickness on the n-Si substrates was achieved by observing the thickness on the digital thickness monitor attached with the evaporation unit.

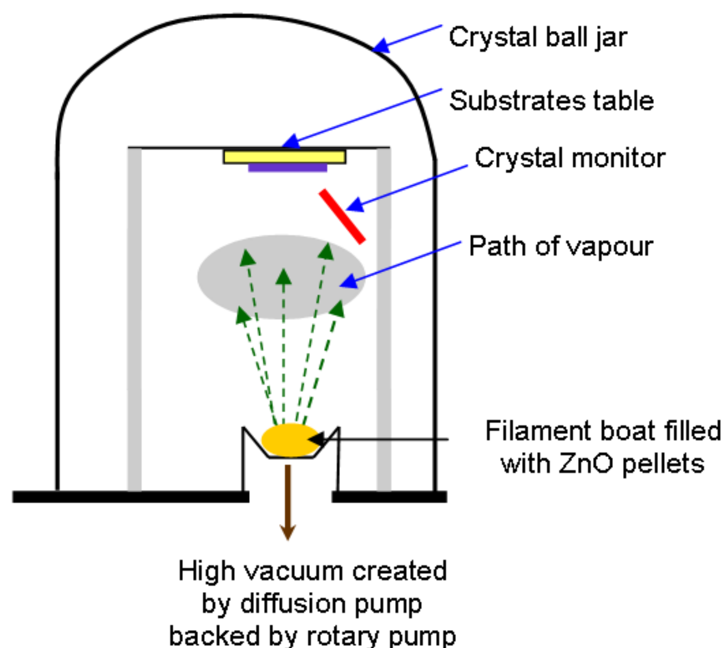

Figure 3.1: Schematic diagram of thermal evaporation process

3.2.3 Annealing of ZnO Films

Annealing is the heat treatment process which is used to alter the material properties of any film by increasing its ductility and thereby making the material more workable [Smith (1994), Rollett *et al*. (2004)]. It involves heating the film (normally in a particular gaseous environment) at a suitable temperature above the critical temperature of the film material and then the film is cooled down to the room temperature. Annealing can induce ductility, soften material, relieve internal stresses, and refine the structure by making it homogeneous [Rollett *et al*. (2004), Periasamy *et al.* (2010)].

In the present work, the ZnO thin film coated n-Si substrates were taken out from the evaporation unit and placed in a furnace for annealing treatment of the as-grown ZnO thin films prepared by the thermal evaporation method discussed above. The ZnO film was heated in the N_2 gas atmosphere at 550 °C for 30 minutes in the Thermo Mini brute model 3-stack diffusion furnace. The furnace was fitted with "Analock" digital temperature controllers to control the temperature of each of the furnaces with an error margin of 0.5 ºC at 1200 ºC. Each tube of the furnaces was equipped with the facility for controlling the flow of desired gases inside it through a flow meter to monitor the rate of flow. The

annealing treatment of ZnO thin film in N_2 gas atmosphere was used to minimize the structural defects in the vacuum deposited ZnO thin film surface thereby improving the crystalline quality of the ZnO films under consideration [Ghafouri *et al*. (2013)]. It may be mentioned that the N_2 at the annealing temperature range of 600-900 °C may act as N_2 acceptors for the single ZnO crystals [Garces *et al*. (2002)]. That is why, the annealing temperature of 550 °C has been chosen for the present study. After annealing treatment, one set of samples were cool down to room temperature for the film characterization purpose while another set of samples were processed for Schottky diode fabrication.

3.2.4 Fabrication of Pd/ZnO Thin Film Schottky Diodes

The annealed ZnO thin film coated n-Si substrates were placed in the thermal evaporation unit under the same conditions of the chamber as were used for the ZnO film deposition. Using Pd foil as source material, Pd metal dots were deposited on the annealed ZnO thin films by using shadow mask technique for fabricating the Pd Schottky contacts on the ZnO films under consideration. The grid shadow masking was used to fix the electrode dimensions of 1mm×1mm and electrode spacing of 5 mm. The thickness monitor of the vacuum coating unit was set at 100 nm. The area of each metal dot was calculated as ~0.785×10^{-2} cm^{-2}. The Ti/Al metal was deposited on the entire back-surface (i.e. opposite to the ZnO film) of the n-Si substrates by the thermal evaporation method. The Ti/Al bilayer metallization is commonly used for the fabrication of an effective ohmic contact on ZnO due to the formation of the intermediate phase of Al_3Ti [Kim *et al*. (2002)]. In order to examine the electrical characteristics of the n-Si/n-ZnO heterojunctions, another set of device was also fabricated by depositing Al and Ti/Al ohmic contacts on the ZnO film and back-surface of the n-Si substrates respectively. After deposition of electrical contacts, the two device structures namely Pd/ZnO thin film/n-Si substrates/Ti/Al Schottky diode and Al/ZnO thin film/ Ti/Al were processed for the post-fabrication annealing treatment in the N_2 environment at 550 °C for 7 min to improve quality of the electrical contacts as suggested by Brillson and Lu (2011). The Schematic diagram of whole fabrication process of the Schottky diode under study is now demonstrated in Fig.3.2.

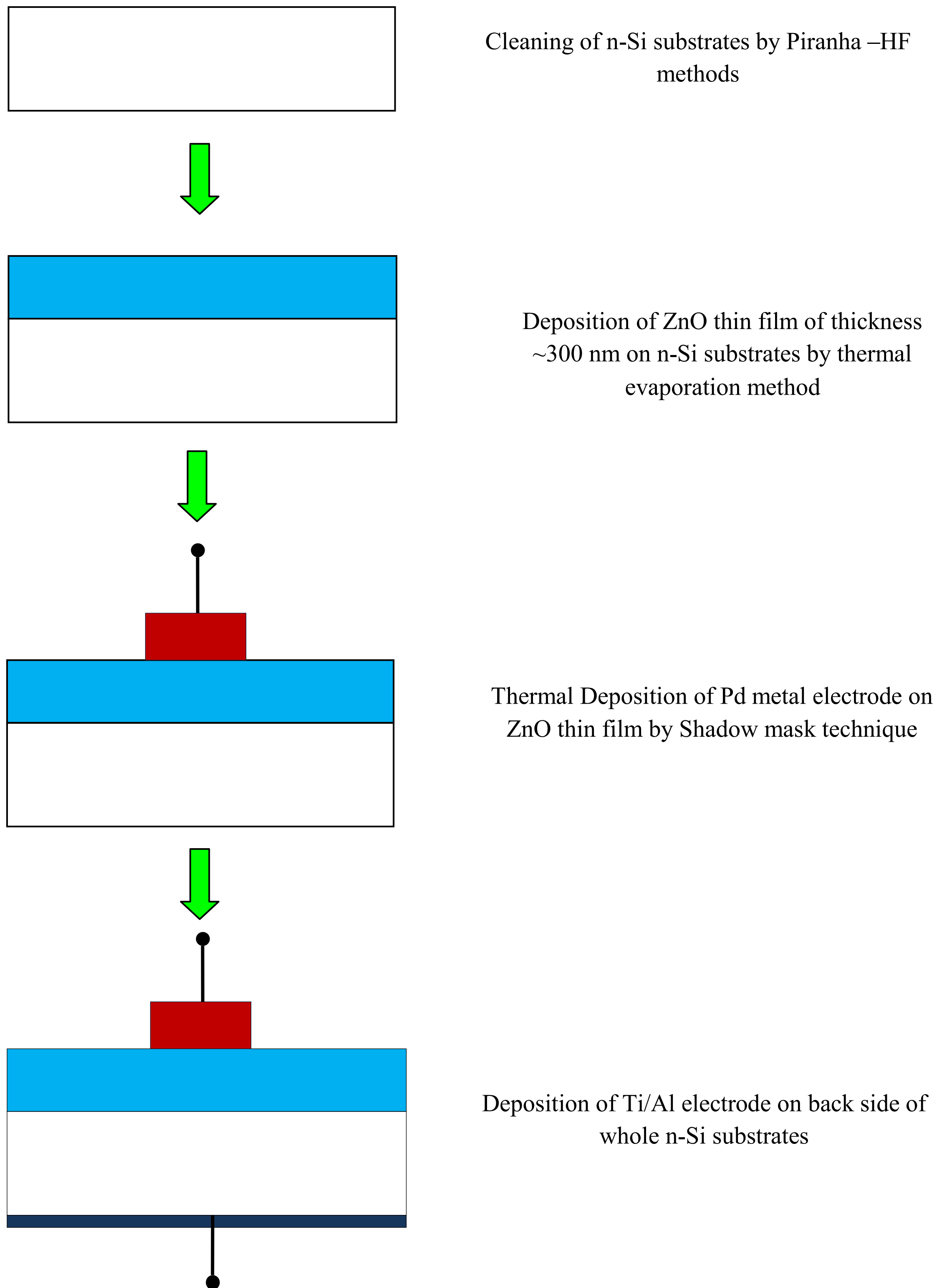

Figure 3.2: Schematic diagram for fabrication details of Pd/ZnO thin film/n-Si/Ti/Al Schottky diodes

3.3. Results and Discussion

In this section, we will present some important results related to the ZnO thin film properties as well as electrical properties of the Pd/ZnO thin film Schottky diodes grown on the n-Si substrates under consideration. We will first start with the discussion related to the morphological and optical characteristics of the ZnO films in the following.

3.3.1 ZnO Thin Film Characterization

3.3.1.1 Surface morphology study by using FESEM image

The surface morphology of the as-grown ZnO thin films on n-Si substrates has been analyzed by using FESEM microscopy (model no.FEI QUANTA 200, FESEM). Fig. 3.3 shows the FESEM image (top view) of the vacuum deposited ZnO thin films on n-Si substrates under consideration. Clearly, the as-grown ZnO thin films have nanocrystalline surface morphology with a homogeneous distribution over the entire substrate's surface.

3.3.1.2 X-ray diffraction pattern

The crystalline structure of the as-grown ZnO thin film has been determined by analyzing the XRD diffraction pattern (model no. XDMAX, PC-20, 18 kW Cu rotating anode, Rigaku, Tokyo, Japan) in continuous scan mode from $2\theta = 30\text{-}60^o$ with a slow scanning speed. Fig. 3.4 shows the XRD spectrum of the ZnO thin films under study. Different intensity peaks (100), (002), (110), (102), (110) at $2\theta =$ 31.81º, 34.43º, 36.25º, 47.50º, 56.66º observed in the XRD spectrum are well matched with the JCPDS data card no.36-1451 of ZnO [JCPDS (1977), Jagadish and Pearton (2006)]. The maximum and minimum intensity peaks among the above five planes are observed at the (101) and (102) diffraction planes respectively. The XRD pattern shows that the as-deposited ZnO thin films have the wurtzite crystal structure with hexagonal phase of ZnO [Jagadish and Pearton (2006)]. However, no clear preferred orientation is observed in the XRD pattern due to the large mismatching between the lattice constants and thermal coefficients of n-Si substrate and those of the ZnO thin films [Shen *et al.* (2006), Wang *et al.* (2007)].

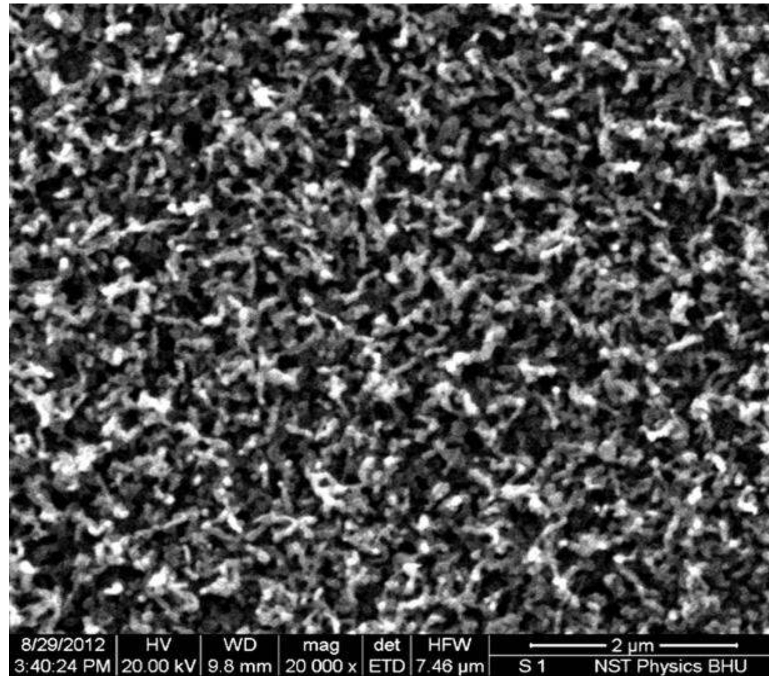

Figure 3.3: FESEM image of ZnO thin film grown on n-Si substrates by thermal evaporation method

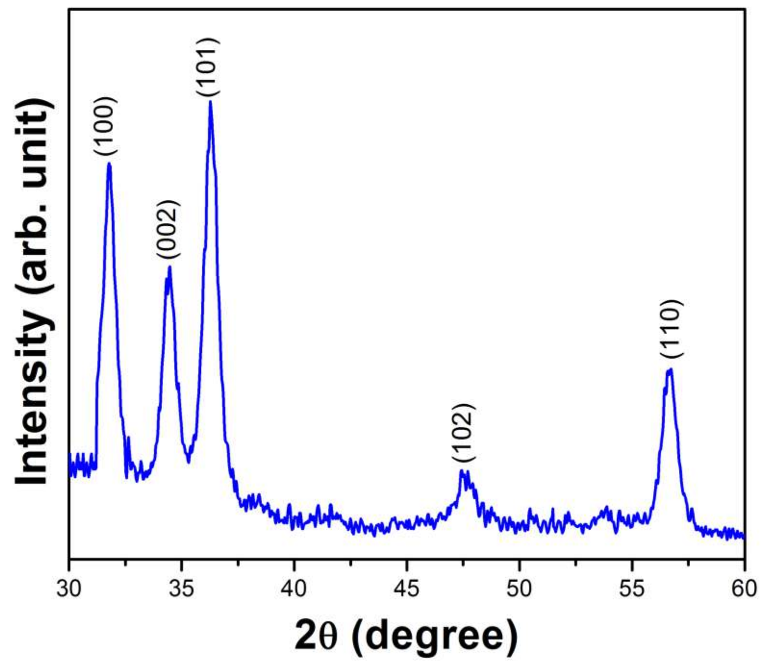

Figure 3.4: Typical XRD pattern of ZnO thin film grown on n-Si substrates

3.3.1.3 Energy dispersive spectrum (EDS) of the ZnO thin film

The chemical composition of ZnO thin films grown on the n-Si substrates have been determined by the energy dispersive spectrum (EDS) as shown in Fig.3.5. A good amount of atomic percentages of Zn and O atoms has been found in the EDS spectrum. The peak of the Si material is also present in the EDS spectrum due to the Si substrate. No peak of any other materials or impurities is observed in the EDS spectrum. This clearly shows that no catalyst metal is involved in the growth of the ZnO thin film.

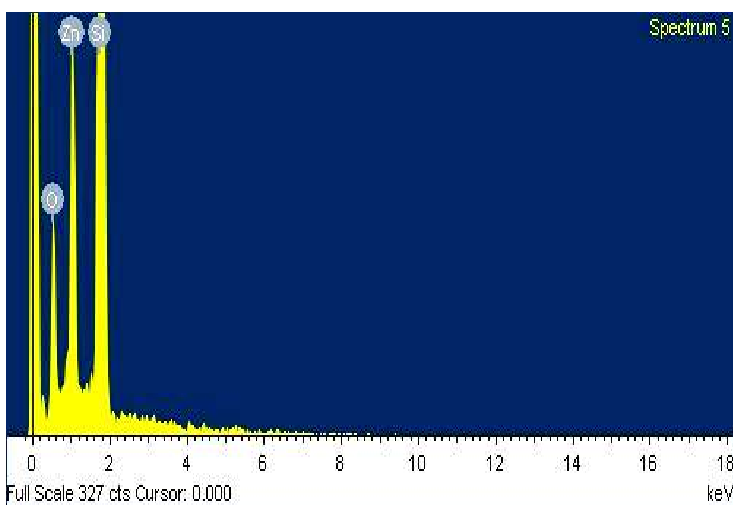

Figure 3.5: Typical EDS spectrum of ZnO thin film grown on n-Si substrates

3.3.2 Photoluminescence (PL) Spectrum of ZnO Thin Film

The methodology of the PL has already been discussed in Chapter.1. In our present work, we have studied the photoluminescence (PL) spectrum (Model: RPM 2000, Accent Optics, USA) of the as-grown ZnO thin films under consideration using the Nd–YAG laser source with 266 nm excitonic wavelength. The PL spectrum of as-grown ZnO thin films is shown in Fig. 3.6. It is observed from the Fig. 3.6 that the vacuum deposited ZnO thin films have strong near band edge (NBE) emission at wavelength of ~380 nm due to the excitonic transition between the valance band and conduction band [Djurišić and Leung (2006), Zhai *et al*. (2009)]. An additional broad emission spectrum over 400-600 nm wavelength range

is also observed in the PL spectrum. This is possibly due to the presence of deep level defects such as Zn interstitial (Zn_i) and oxygen vacancies (V_0) in the band gap of ZnO.

It may be mentioned that the defect related emissions depend upon the crystal quality. A good quality ZnO crystal normally shows enhanced UV emission characteristics with a reduced level of the deep level emissions [Djurišić and Leung (2006), Biswas (2010)]. Thus the PL spectrum shown in Fig. 3.6 clearly demonstrates that the ZnO films under consideration are of a good quality with a dominant UV emission peak. The undoped ZnO thin films under study usually contain various intrinsic defects such as Zn vacancies, oxygen vacancies, interstitial Zn, antisite oxygen and interstitial oxygen [Teng *et al.* (2006), Fang *et al.* (2010)] as already mentioned in Chapter 1. These intrinsic defects form either donor level or acceptor level in the bandgap and thereby greatly affecting the electrical and optical properties of ZnO thin film based devices.

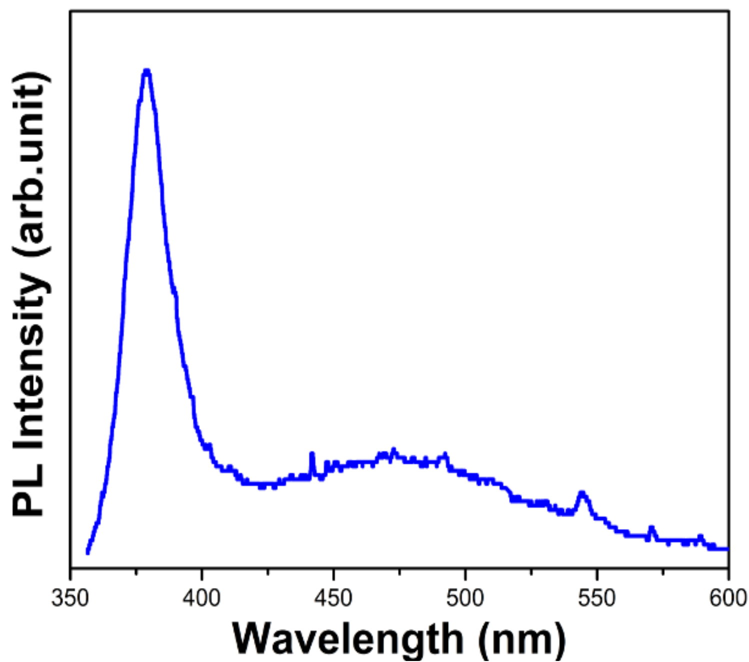

Figure 3.6: PL spectrum of ZnO thin film grown on n-Si substrates by thermal evaporation method

3.3.3 Energy Band Diagram

Fig. 3.7 shows the energy band diagram of the Pd/ZnO thin film Schottky diodes fabricated on n-Si substrates by the thermal evaporation method as discussed earlier. From the

Schottky-Mott theory [Schottky (1938)], the ideal barrier height is given by $\phi_{B,eff}(eV) = \phi_m(eV) - \chi(eV)$ which is normally much lower in the practical Schottky devices due to presence of interface states and barrier inhomogeneities at the metal/semiconductor interface. The current transport across the n-ZnO/n-Si junction is determined by transfer of electron over band offset as discussed in Chapter 1. The value of conduction band offset $\Delta E_C = \chi_{ZnO} - \chi_{Si}$ is equal to 0.35 eV and the value of valence band offset is calculated as $\Delta E_V = (E_{ZnO} - E_{Si}) - \Delta E_C$ ~1.8 eV. The larger value of the valence-band offset than the conduction-band offset prevents the movement of holes from Si to ZnO [Sze (1981)].

On the other hand, the small conduction band offset may result in the current across the n-ZnO/n-Si junction due to the flow of electrons from the n-ZnO to the n-Si side and vice versa. The current across Pd/ZnO interface is mainly determined by the thermionic emission of electrons from the ZnO semiconductor to Pd metal over the built-in potential barrier at the Pd/ZnO interface similar to that of any other Schottky junction [Sze (1981)]. It should be noted here that the depletion width as well as the band bending near the n-ZnO/n-Si interface will be negligible due to the ohmic nature of the junction as shown later in this section.

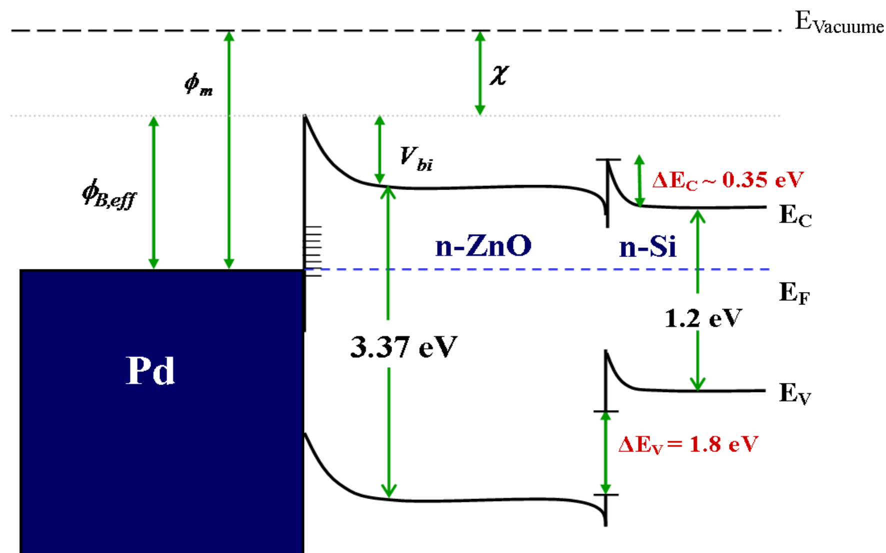

Figure 3.7: Energy band diagram of Pd/ZnO/n-Si Schottky diodes

3.3.4 Electrical Characteristics of Pd/ZnO Thin Film Based Schottky Diodes Grown on n-Si Substrates

After investigation the properties of the ZnO films, we will now discuss the electrical characteristics of the Al/ZnO thin film/n-Si/Ti/Al and Pd/ZnO thin film/n-Si/Ti/Al devices in the following.

3.3.4.1 Electrical characteristics of n-ZnO/n-Si contacts

The electrical characteristics of n-ZnO/n-Si contact have been determined by depositing Al metal dot on front side of ZnO thin film and Ti/Al metal on back side of whole n-Si substrates by thermal evaporation method as already mentioned in fabrication details. The I-V characteristics of the Al/n-ZnO thin film/n-Si/Ti/Al have been measured by using a semiconductor parameter analyzer (Agilent B1500A) as shown in Fig. 3.8 in the voltage range from -2 to +2 V. The nearly linear I-V characteristics of the Al/n-ZnO thin film/n-Si/Ti/Al structure clearly show the nearly ohmic nature of n-ZnO/n-Si heterojunction on which the Schottky diodes under consideration have been fabricated. The ohmic nature of n-ZnO/n-Si shown in Fig. 3.8 further confirms that the n-Si/Ti/Al contact can be used to work as an effective cathode electrode for ZnO thin film in the proposed Schottky device structure under consideration in the present chapter.

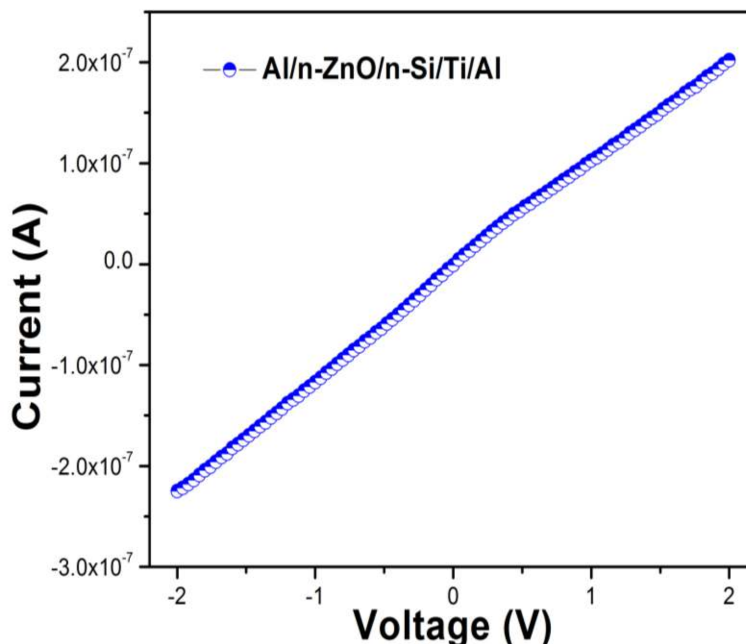

Figure 3.8: I-V characteristics of n-ZnO/n-Si contacts

3.4.1.2 Room temperature capacitance-voltage (C-V) characteristics

The C-V characteristics of the Pd/ZnO thin film Schottky contacts grown on n-Si substrates have been measured by using a microprobe station attached with computer controlled impedance analyzer (HP-4284A, LCR meter) in the voltage range between -2 to +2 V at room temperature. It may be mentioned here that the C-V characteristics of the Schottky diodes are extremely sensitive to the low frequencies of the ac signals used for the C-V measurements. The interface states at the Pd/ZnO interface can directly follow the slow variation in the ac signals [Aydoğan *et al.* (2009), Hussain *et al*. (2012)]. However, the interface states are found to be almost insensitive to ac signals of high frequencies (~1MHz), and hence have negligible effect on the C-V characteristics [Werner (1988), Chattopadhyay and Haldar (2001)]. In view of the above, the C-V characteristic at only 1MHz frequency (as shown in Fig. 3.9) is considered in the present study.

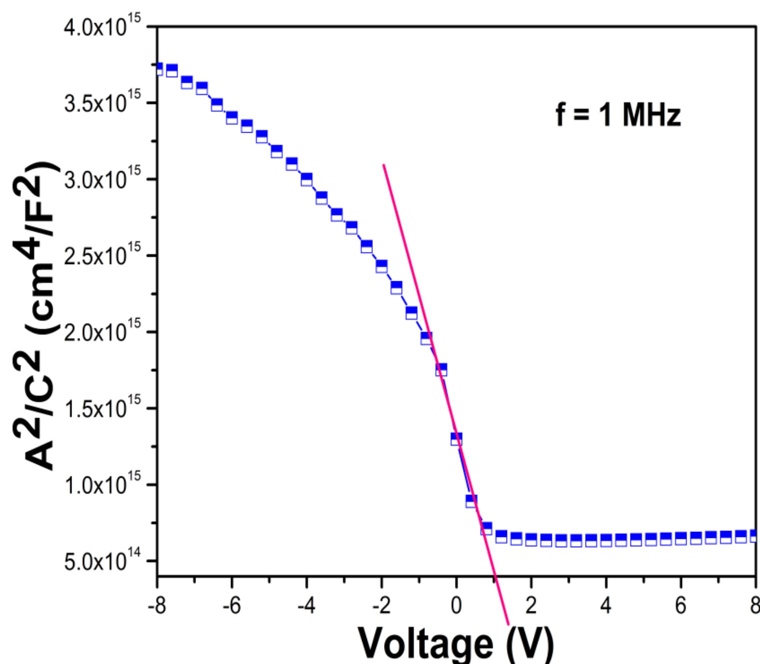

Figure 3.9: A^2/C^2 versus V characteristics of Pd/ZnO thin film based Schottky diodes

For Pd/ZnO thin film Schottky junction under discussion, the C-V characteristics can be described by the relation [Sze (1981), Rhoderick and William (1988)]

$$\frac{A^2}{C^2} = \frac{2\left(V_{bi} - V - \frac{kT}{q}\right)}{qN_D\varepsilon_s} \tag{3.1}$$

where A is the junction area, N_D is the donor concentration of n-ZnO, $\varepsilon_s(=9.0\varepsilon_0)$ is the permittivity of the n-ZnO, V is the applied bias voltage and V_{bi} is the built in potential of the junction. Eq. (3.1) shows that the A^2/C^2 versus V should be a linear curve whose intercept with the applied bias voltage axis (V) provides the value of $(V_{bi} - kT/q)$ and the slope (say, *m*) can be used to estimate the doping concentration N_D of ZnO by using the following relation:

$$N_D = \frac{2}{mq\varepsilon_s} \tag{3.2}$$

The measured values of A^2/C^2 have been plotted against the applied bias voltage in Fig.3.9. Extrapolating the linear segment of the A^2/C^2 vs. V curve to the applied voltage axis, the value of the built-in potential is estimated as V_{bi} ~1.15 eV. Further, using the slope of the linear segment of A^2/C^2 versus V, the value of N_D is computed from Eq. (3.2) as 2.16×10^{15} cm^{-3}.

Now, the value of the barrier height at Pd/ZnO thin film interface can be estimated by using the following relation [Sze (1981), Hussain *et al*. (2012)].

$$\phi_{B,eff}^{C-V} = V_{d0} + V_n \tag{3.3}$$

where $V_{d0} = V_{bi} + kT/q$ is the diffusion voltage at zero bias and

$$V_n = \frac{kT}{q} ln\left(\frac{N_C}{N_D}\right) \tag{3.4}$$

represents the depth of the Fermi level below the conduction band in the neutral region of the ZnO film where $N_C = 3.5\times10^{18}\ cm^{-3}$ is the effective density of states in the conduction band of ZnO with $m_e^* = 0.27\ m_0$ as the effective mass of the electron [Sze (1981), Hussain *et al*. (2012)]. The barrier height of the Pd/ZnO Schottky contacts under study estimated from the C-V measurements using Eq. (3.3) is determined as 1.36 eV.

3.3.4.3. Room temperature current (I)-voltage (V) characteristics of Pd/ZnO thin film Schottky diodes grown on n-Si substrates with series resistance

The room temperature current (I)-Voltage (V) characteristics of Pd/ZnO thin film Schottky diodes grown on n-Si substrates have been shown in Fig 3.10. The I-V characteristics have been measured by the semiconductor parameter analyzer (Agilent B1500A) in the voltage range from -2 to +2V as shown in the Fig 3.10. The as-fabricated Schottky diodes shows a good rectification ratio (i.e. the ratio of the forward current I_F measured at 2V and reverse current I_R at the same reverse bias voltage of –2 V) of $I_F / I_R = 1.13\times10^2$ under dark condition.

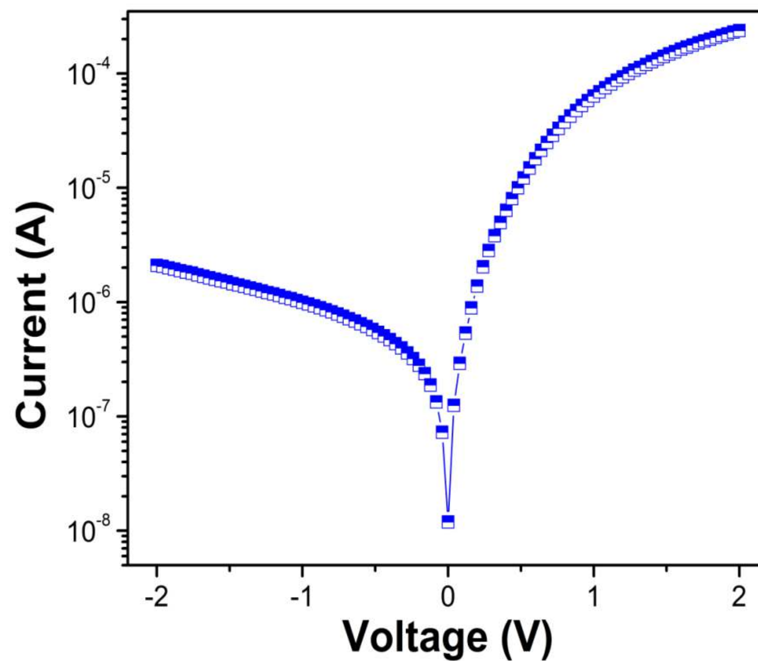

Figure 3.10: Room temperature I-V characteristics of Pd/ZnO thin film Schottky diodes grown on n-Si substrates by thermal evaporation method

The downward concave curvature of the forward bias I-V plot (shown in Fig 3.10) at sufficiently large voltages is mainly caused by the series resistance R_s mainly resulted from the base (substrate) material of the diode [Norde (1979)]. Thus, in order to estimate the electrical parameters of the Pd/ZnO Schottky diode accurately, the measured I-V characteristics must be analyzed by taking the effect of series resistance into account as discussed in the following. According to the thermionic emission theory [Bethe (1942)],

the forward current at the Pd/ZnO thin film Schottky junction can be expressed by the following relation [Mead (1965), Sze (1981), Rhoderick and Williams (1988]

$$I = I_0\left\{= AA^*T^2\, exp\left(-\frac{q\phi_{B,eff}}{kT}\right)\right\} exp\left(\frac{q(V - IR_s)}{\eta kT}\right) \quad (3.5)$$

where q is the elementary charge, V is the applied voltage, η is the ideality factor, k is the Boltzmann constant, R_s is the series resistance, A is the contact area, A^* is the effective Richardson constant of ZnO, T is the absolute temperature, I_0 is the reverse saturation current and $\phi_{B,eff}$ is the effective barrier height (in volt) at zero bias. As discussed in Chapter-1, $\phi_{B,eff}$ is defined as

$$\phi_{B,eff} = \frac{kT}{q} ln\left(\frac{AA^*T^2}{I_0}\right) \quad (3.6)$$

The value of the reverse saturation current I_0 can be calculated from the extrapolated intercept of $ln\, I$ vs. V plot with the current axis for $V = 0$ as discussed in Chapter-1. From the measured I-V characteristics shown in Fig.3.10, we can obtain $I_0 \sim 8.76\times10^{-8}$ A . The value of I_0 is then used in Eq. (3.6) to determine the value of $\phi_{B,eff}$ as 0.67 eV.

Note that the ideal value of the barrier height of Pd/ZnO Schottky contacts obtained from the Schottky-Mott theory [Sze (1981)] varies from **0.77 eV** (with work function (ϕ_M) of Pd as 5.12 eV [Wenckstern *et al.* (2006)] and electron affinity (χ) of ZnO as 4.35 eV [Majumdar and Banerji (2009)]} to **1.42 eV** (with $\phi_M = 5.12$ eV and $\chi = 3.7 eV$ [Sze (1981)]. Such deviation of the barrier height from its ideal value is mainly caused by the presence of high surface states or band bending in ZnO itself as pointed out by Bardeen [Bardeen (1947)] and Neville and Mead [Neville and Mead (1970)]. It may be mentioned that the value of barrier height obtained from the room temperature C-V measurements is also higher than the room temperature I-V measurements.

Now, the value of the ideality factor (η) is calculated from the slope of the linear region (i.e. low current region) of the forward bias shown in Fig. 3.10. From the discussion of Chapter-1, η is rewritten as

$$\eta = \frac{q}{kT}\left(\frac{dV}{d\, ln(I)}\right) \quad (3.7)$$

From the Eq. 3.7, the value of η is estimated as ~2.36 which is much larger then unity. The high values of η is attributed to the presence of the interfacial thin oxide layer, a wide distribution of low- Schottky barrier height (SBH) patches and the bias voltage dependence of the SBH [Werner and Güttler (1991)] as discussed in Chapter-1.

Determination of Series Resistance: We will now determine the series resistance of the Schottky diodes under consideration. The equivalent circuit of Schottky diodes with series resistance R_s is shown in Fig. 3.11. To determine the effect of R_s on the device parameters, let us consider a small current region of the forward bias I-V characteristics of the Schottky diodes where $I \sim I_0$ and $IR_s << 3kT/q$. For any applied voltage $V > 3kT/q$ but $IR_s << 3kT/q$ (i.e. negligible as compared to V), the junction voltage becomes $V - IR_s \approx V$ and thus Eq. (3.5) is reduced to the following equation [Sze (1981)]:

$$I \approx I_0 \left\{ exp\left(\frac{qV}{\eta kT}\right) - 1 \right\} \approx I_0 \, exp\left(\frac{qV}{\eta kT}\right) \quad for\ V > \frac{3kT}{q} \tag{3.8}$$

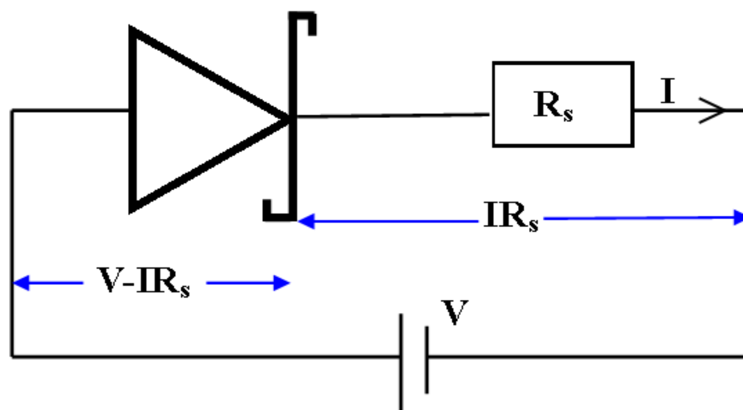

Figure 3.11: Equivalent circuit of Schottky diodes with series resistance

From the above discussion, it is clear that the series resistance R_S has virtually no effect on the estimated parameters I_0, η and ϕ_{Beff} since they are estimated in the low current region where $I \sim I_0$. However, R_s may play a significant role in determining the diode characteristics in the high current region where the IR_s voltage drop can't be

neglected with respect to the applied bias voltage V [Norde (1979), Cheung and Cheung (1986)].

According to Tung [Tung (1992)], the I-V characteristics of the Schottky contacts are linear in the semi-log scale at low forward bias voltage but become significantly non-linear in nature at higher forward bias voltages due to the series resistance R_s resulted from the base (substrate) material. Clearly, while R_s have very small effect in the low forward bias region, it has significant effect in the higher current region due to the significant voltage drop IR_s. In order to determine the value of the series resistance of the device, we will compare the three methods discussed below:

(a)Direct Method: The dynamic resistance defined by $R_i = \frac{dV}{dI}$ [Pür and Tataroğlu (2012)] has been plotted as a function of the applied bias voltage V as shown in Fig.3.12.

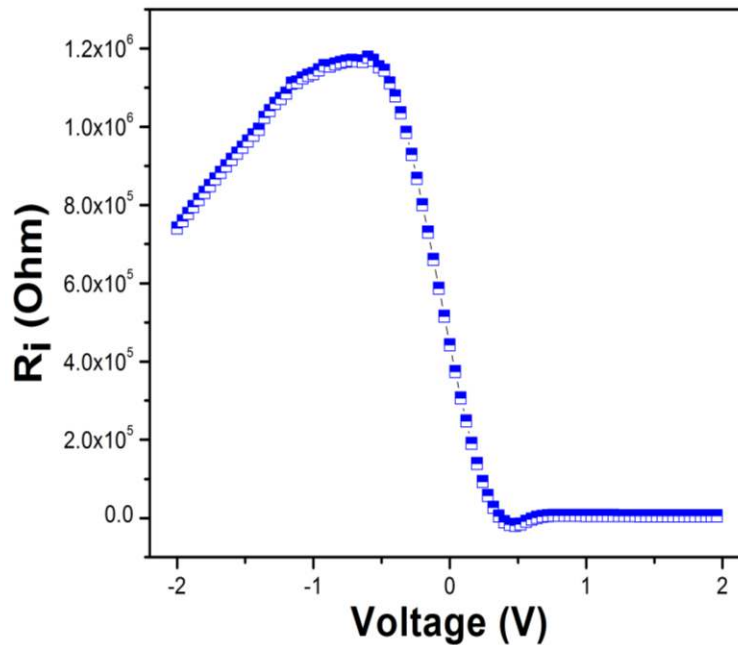

Figure 3.12: Plot of the bias-dependent resistance $R_i = \frac{dV}{dI}$ versus applied voltage

It is observed from Fig.3.12 that while the dynamic resistance of the diode varies with the applied reverse bias voltage for $V < 1.5\text{V}$, a nearly bias-independent constant value of the $R_i \sim 5333\Omega$ is observed for higher voltages (i.e. $V > 1.5\text{V}$). Since the series resistance is

mainly manifests at higher bias region where the voltage drop IR_s is much larger than the voltage appearing across the diode, the value of $R_i \sim 5333\Omega$ for $V > 1.5\text{V}$ represents the series resistance R_s of the Schottky diodes under consideration. However, the method is not an accurate one as compared to the following two methods.

(b)Determination of the Series Resistance by Using Cheung's function: In the direct method discussed above, the effects of R_s on the determination of barrier height and ideality factor were neglected. We now consider the more accurate method proposed by Cheung and Cheung in 1986 [Cheung and Cheung (1986)] to determine the $\phi_{B,eff}$, η and R_s from the forward bias measured I-V data by using the following relations:

$$\frac{dV}{d(ln\,I)} = \frac{\eta kT}{q} + IR_s \tag{3.9}$$

$$H(I) = V - \left(\frac{\eta kT}{q}\right) ln\left(\frac{I}{AA^{*}T^{2}}\right) \tag{3.10}$$

$$H(I) = \eta\phi_{B,eff} + IR_s \tag{3.11}$$

The slope of the plot of $dV / d(ln\,I)$ vs. I shown in Fig. 3.13 (a) gives the value of the series resistance $R_s = 4734$ Ω. Now, equating the intercept of the plot at zero-current axis to $\eta kT/q$, the value of η is determined as ~5.79. In the Fig. 3.13 (a), the black hollow squares represent the experimental data whereas the solid line represents their linear fit. Note that the value of η is much larger than the value η =2.36 determined by using the conventional ($ln\,I$ vs. V) method described by Eq.(3.6) which is attributed to the voltage drop across the series resistance and presence of interface states.

The presence of series resistance $R_s = 4734$ Ω in the Pd/ZnO Schottky diode makes the diode more non-ideal in nature thereby increasing the value of η. By using the value of η in Eq. (3.11), we have drawn the plot of $H(I)$ vs. I in Fig. 3.13 (b). The value of R_s is now estimated from Fig. 3.13 (b) as 4734 Ω which is again same as that obtained from Fig. 3.13 (a). The value of $\phi_{B,eff}$ is estimated from Fig. 3.13 (b) as ~0.668eV which closely agrees with that obtained from the conventional method using the linear (i.e. low current) region of the experimental $ln\,I$ vs. V plot discussed earlier.

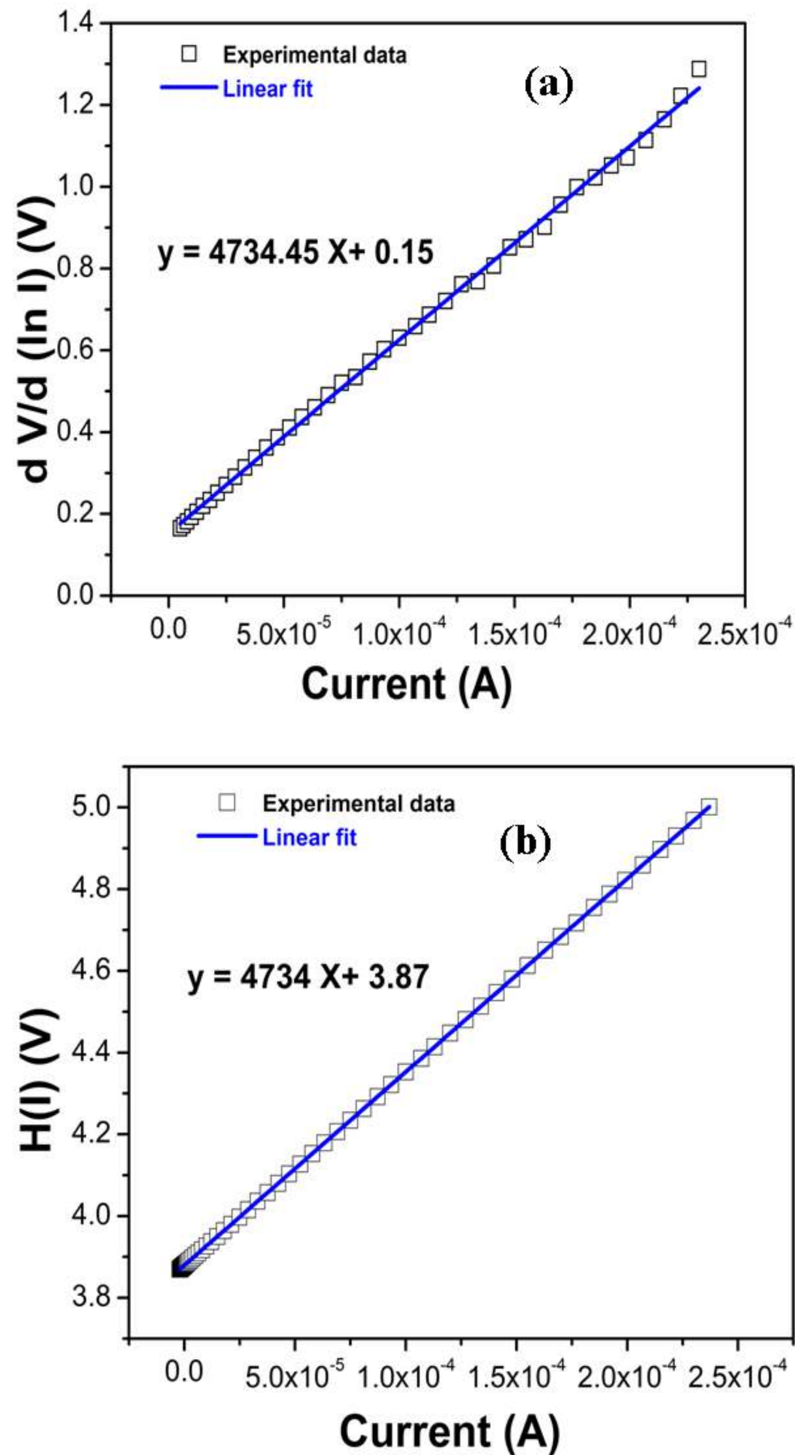

Figure 3.13: **(a)** Plot of dV/d ln (I) versus I **(b)** plot of H (I) vs. I for Pd/ZnO thin film Schottky diodes grown on n-Si substrate

(c) Norde's method: We will now determine the value of the series resistance by using the Norde's function described by the following relation [Norde (1979), Aydoğan *et al.* (2009)]:

$$F(V) = \frac{V}{\gamma} - \frac{kT}{q}\ln\left(\frac{I(V)}{AA^{*}T^{2}}\right) \tag{3.12}$$

where $\gamma\,(=3)$ is the smallest integer (dimensionless) greater than $\eta\,(\sim 2.36)$ measured from the conventional method.

Using measured values of the I-V characteristics, the variation of $F(V)$ as a function of the applied bias voltage V is shown in Fig.3.14. According to the Norde's method, the value of the barrier height is given by [Şahin *et al*. (2005), Faraz *et al*. (2012)]

$$\phi_{B,eff} = F(V_0) + \frac{V_0}{\gamma} - \frac{kT}{q} \tag{3.13}$$

where $F(V_0)$ is the minimum point of $F(V)$ occurring at $V = V_0$. The value of R_s for Pd/ZnO thin film contacts grown on n-Si substrates has been determined by using the following relation [Norde (1979), Aydoğan *et al.* (2009)]:

$$R_s = \frac{kT(\gamma - \eta)}{qI_{min}} \tag{3.14}$$

where I_{min} is the minimum current corresponding to voltage V_0 at which $F(V)$ possesses its minimum value as also depicts in Fig 3.14. From the F - V plot, we obtain $F(V_0)$= 0.67 V and V_0 = 0.12 V. The value of the $\phi_{B,eff}$ and R_s are calculated from Eq. (3.13) and (3.14) as 0.68 eV and 30.983×10^3 Ω respectively.

Finally, we have summarized the values of all parameters such as the barrier height, ideality factor and series resistance obtained by the conventional method, Cheung's function and Norde's method in Table 3.1. The conventional thermionic emission analysis (i.e. conventional method) gives barrier height ~0.67 eV, ideality factor ~2.36 and series resistance ~5333 Ω. The Cheung's method has resulted in a nearly same barrier height of ~0.67eV but a much larger value of ideality factor ~5.29 and a relatively smaller value of series resistance ~4734 Ω as compared to the conventional method. The Norde's method gives the nearly same value of the barrier height of ~0.67eV but a much larger value of the series resistance R_s~30.983×10^3 Ω than the other two approaches. It may be mentioned

that Norde's model is based on the assumption that the Schottky diodes have an ideality factor of unity. Thus, the large value of R_s obtained from the Norde's model is attributed to the non-suitability of the Norde's model for Schottky diodes with $\eta > 1$. The study also shows that Cheung's method could be the best and most practical for estimating the diode parameters including the effect of series resistance of the Pd/n-ZnO thin film/n-Si Schottky diode structures under consideration.

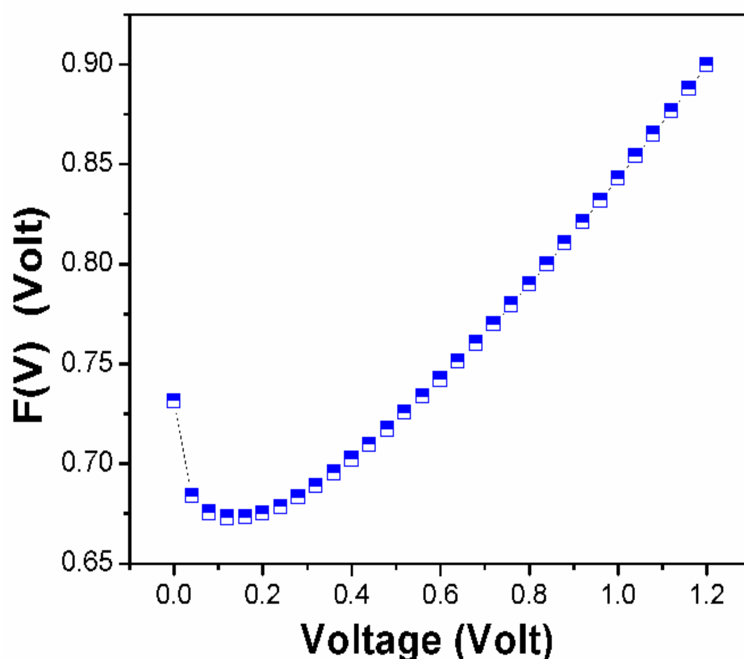

Figure 3.14: F(V) vs. V plot for Pd/ZnO thin film Schottky contacts

Table.3.1 Shows different electrical parameters of Pd/ZnO Schottky diode grown on n-Si substrates by using different methods.

Device parameters	Conventional Method	Cheung-Cheung method		Norde's method
		d V/d (lnI) vs. I	H(I) vs. I	
Barrier height (eV)	0.67	-	0.67	0.68
Ideality factor	2.36	5.79	-	-
Series resistance (Ω)	5333	4734.45	4734	30.983×10^3

3.3.4.5 Temperature-dependent current-voltage (I-V-T) characteristics of Pd/ZnO thin film Schottky diodes grown on n-Si substrates

The temperature-dependent I-V characteristics of Pd/ZnO thin film Schottky diodes grown on n-Si substrates measured in the voltage range from -2 to +2V have been shown in Fig. 3.15. The I-V characteristics have been measured by using the semiconductor parameter analyzer (Agilent B1500A) in the temperature range of 300-423 K selected arbitrarily on the basis of the limitation of our measurement set-up. The sample temperature was always monitored by using a Temptronic (Model no.TP-36 B) thermo chuck C-V plot system. It is clearly observed from Fig.3.15 that the observed I-V characteristics are strongly dependent on the operating temperature of the Pd/ZnO thin film Schottky diodes under consideration in this chapter. Following the conventional method, the values of the reverse saturation current (I_0), barrier height $(\phi_{B,eff})$ and ideality factor (η) have been estimated and listed in Table 3.2 for different operating temperatures in the range of 300-423 K.

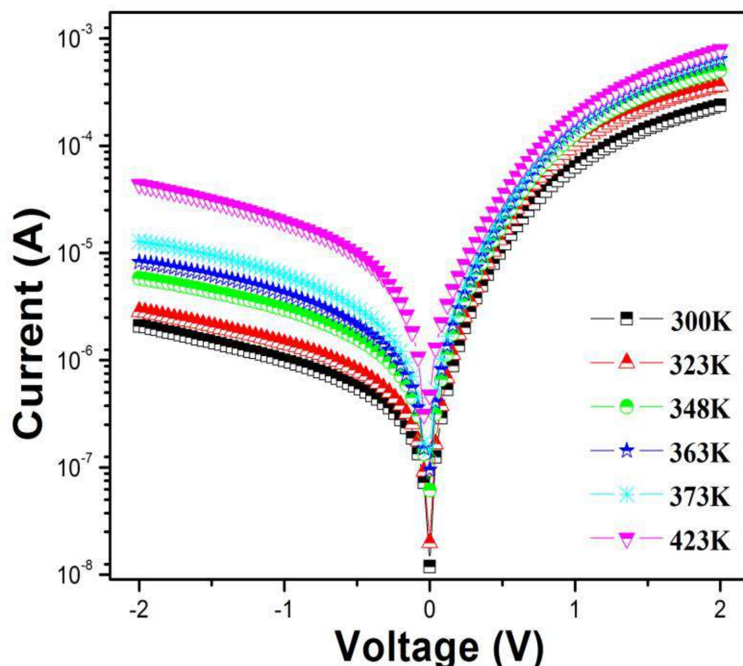

Figure 3.15: Temperature- dependent I-V characteristics of Pd/ZnO thin film Schottky contacts grown on n-Si substrate for a operating temperature range of 300-423 K

Table. 3.2 Calculation of reverse saturation current, barrier height, and ideality factor for the Pd/n-ZnO thin film Schottky diode grown on n-Si substrates

T (K)	I_0 (A)	$\phi_{B,eff}$ (V)	η
300	8.76×10^{-8}	0.67	2.36
323	1.61×10^{-7}	0.71	2.13
348	2.03×10^{-7}	0.77	1.94
363	3.12×10^{-7}	0.79	1.87
373	4.56×10^{-7}	0.80	1.81
423	1.13×10^{-6}	0.89	1.48

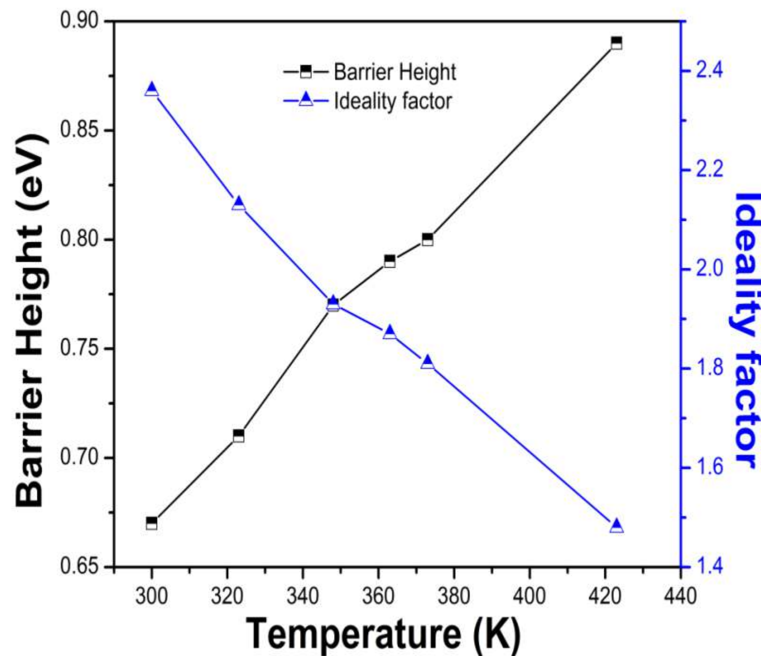

Figure 3.16: Variation of barrier height and ideality factor with temperature

It may be observed from Table. 3.2 that the value of the $\phi_{B,eff}$ is increased from 0.67 eV to 0.89 eV whereas the value of η is decreased from 2.36 to 1.48 (η>1) with corresponding increase in the operating temperature from 300 to 423K. The variations of $\phi_{B,eff}$ and η with temperature have been shown in Fig.3.16. The similar trends in ZnO based Schottky contacts have also been reported by other researchers [Mtangi *et al*. (2009),

Allen *et al*. (2009), Lajn *et al*. (2009)]. Such variations of barrier height and ideality factor with temperature (300 to 423K) show that current transport across Pd/ZnO interface is a temperature activated process. Since barrier height is randomly distributed due to the barrier inhomogeneity phenomenon [Werner and Güttler (1991)] discussed in Chapter-1, current at lower temperatures is contributed by the electrons surmounting the patches of lower Schottky barrier heights due to their smaller kinetic energy. As a result, the measured barrier height is smaller and ideality is higher at lower temperature. However, as the operating temperature of the device is raised, the electrons gain larger kinetic energy to surmount higher barrier heights thereby resulting in higher values of the measured barrier heights and lower values of the ideality factor at higher temperatures as already discussed in details in Chapter-1.

In order to confirm the existence of the barrier inhomogeneity phenomenon at the Pd/ZnO interface, the variation of $\phi_{B,eff}$ as a function of η has been shown along with its least-squares fit in Fig. 3.17. According to Schmitsdorf *et al.* [Schmitsdorf *et al*. (1997)], the linear relationship between the $\phi_{B,eff}$ and η clearly demonstrates the existence of the lateral inhomogeneities of barrier heights across the Schottky interface.

Now, we determine the value of Richardson constant from temperature dependent I-V characteristics without considering the effect of barrier inhomogeneity phenomenon as mentioned above. For this, we have shown the Richardson plot of $ln(I_0/T^2)$ vs. q/kT in Fig 3.18 showing the thermal activated behavior over the whole temperature range from 300 to 423K. The Richardson constant (A^*) can be determined from the intercept of the graph with the $\ln(I_0/T^2)$ axis. The non-linear characteristics of the $ln(I_0/T^2)$ versus q/kT plot in Fig. 3.18 also confirms the presence of spatial barrier inhomogeneities [Schmitsdorf *et al*. (1997), Sarpatwari *et al*. (2009)] at the Pd/ZnO interface already observed in Fig. 3.17. However, using the intercept mentioned above, the value of the Richardson constant is determined as $6.22\times10^{-8}\,Acm^{-2}K^{-2}$ which is much lower than the theoretically predicated value of $\sim 32Acm^{-2}K^{-2}\,(\text{for}\, m_e^* = 0.27m_0)$ [Mtangi *et al*. (2009), Allen *et al*. (2009)] of the ZnO. The discrepancy between the theoretical and experimental values of the barrier height and Richardson constant can be optimized by taking the effects of barrier inhomogeneities into consideration as discussed in the following.

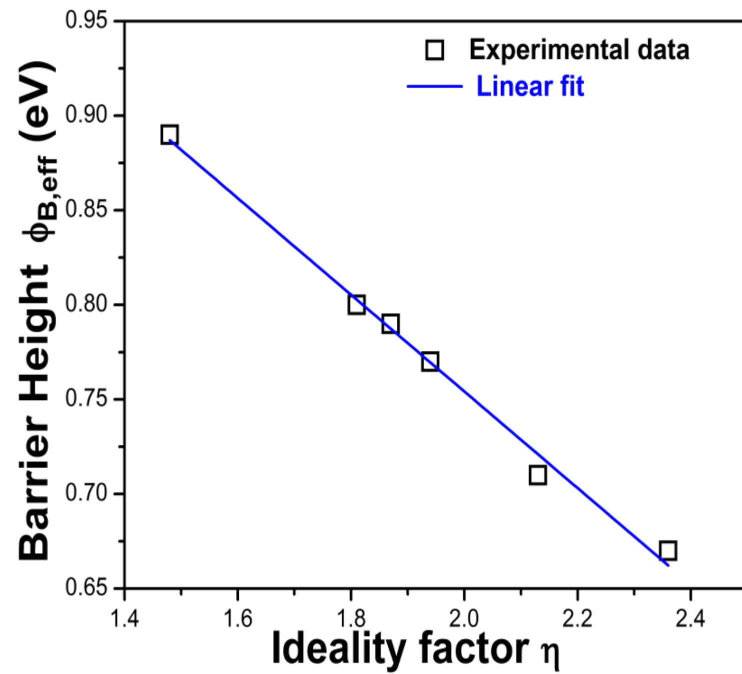

Figure 3.17: Variation of barrier height with ideality factor

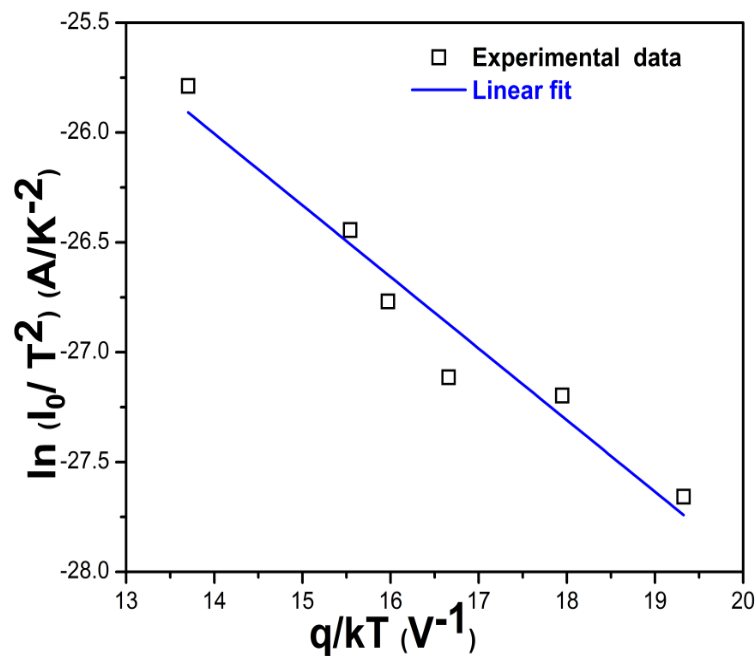

Figure 3.18: Typical $ln(I_0 / T^2)$ versus q / kT plot for determination of experimental Richardson constant without taking the barrier inhomogeneity effects into consideration

3.3.4.6 Determination of mean barrier height and Richardson constant of Pd/ZnO thin film Schottky contacts grown on n-Si substrates including the barrier inhomogenity phenomenon

In order to incorporate the effects of barrier inhomogeneities [Werner and Güttler (1991), Tung (1992), Mönch (1999), Schmitsdorf *et al*. (1997), Dökme *et al*. (2006)] at the Pd/ZnO thin film Schottky contact on the diode parameters, the temperature-dependent I-V results have been analyzed by using the Gaussian function with a standard deviation σ_0 around a mean barrier height $q\phi_{B0,m}$ for the random barrier height distribution [Mtangi *et al*. (2009), Allen *et al*. (2009), Lajn *et al*. (2009)] as discussed in Chapter-1. Note that the subscript '0' is used to denote the zero-bias (i.e. thermodynamic equilibrium condition) of the junction.

Now, following the methodology described by Werner and Güttler [Werner and Güttler (1991)], we now rewrite the following relations from Chapter-1:

$$\phi_{B,eff}(T) = \phi_{B0,m}(T=0) - \frac{q\sigma_0^2}{2kT} \tag{3.15}$$

$$\left(\frac{1}{\eta(T)} - 1\right) = \rho_1 - \frac{q\rho_2}{2kT} \tag{3.16}$$

$$\phi_{B,m}(V) = \phi_{B0,m} + \rho_1 V \tag{3.17}$$

$$\sigma^2(V) = \sigma_0^2 + \rho_2 V \tag{3.18}$$

where $\eta(T)$ is temperature-dependent ideality factor, $\phi_{B,m}(V)$ is the bias-dependent mean barrier height (in volt), $\sigma(V)$ is bias-dependent standard deviation and; ρ_1 and ρ_2 are voltage coefficient which may be dependent on temperature (T) and quantify the voltage deformation of barrier height distribution.

Using the experimental values of $\phi_{B,eff}$ and η from Table-3.2 for different temperatures, we can obtain the $\phi_{B,eff}(T)$ vs. $q/2kT$ and $\left(\eta^{-1}(T)-1\right)$ vs. $q/2kT$ plots as shown in Fig.3.19. Comparing the linear approximation of the $\phi_{B,eff}(T)$ vs. $q/2kT$ plot shown in the Fig. 3.19 with Eq. (3.15), we obtain the zero-bias mean barrier height $q\phi_{B0,m}(T=0) = 1.41\,\text{eV}$ and standard deviation $\sigma_0 = 0.197\,V$. Similarly, assuming that ρ_1

and ρ_2 are independent of temperature [Werner and Güttler (1991)], the $(\eta^{-1}(T)-1)$ vs. $q/2kT$ plot can be approximated as a linear function of $q/2kT$ and compared with Eq. (3.16) to determine ρ_1 = -0.23896V and ρ_2 = -0.04296 V.

It may be noted that the estimated value of the zero-bias mean barrier height $q\phi_{B0,m}(T=0)=1.41eV$ is nearly equal to its theoretical value of 1.42 eV computed from the ideal Schottky-Mott theory by using the work function of Pd as 5.12 eV [Wenckstern *et al*. (2006)] and electron affinity of ZnO as 3.7 eV [Majumdar and Banerji (2009)]. Note that the barrier height 1.41 eV measured from the temperature-dependent I-V characteristics also closely agrees with the value of 1.36 eV obtained from C-V measurements.

Now, taking barrier inhomogeneity correction into the Richardson plot, the modified Richardson activation energy relation is re-written from Chapter-1 as [Zhu *et al*. (2000), Mtangi *et al*. (2009), Hazra and Jit (2014)]

$$ln\left(\frac{I_0}{T^2}\right)-\left(\frac{q^2\sigma_0{}^2}{2(kT)^2}\right)=ln\left(AA^*\right)-\frac{q\phi_{b0,m}(T=0)}{kT} \tag{3.19}$$

The modified $ln(I_0/T^2)-q^2\sigma_0{}^2/2(kT)^2$ vs. q/kT plot has been shown in Fig.3.20. Comparing the plots shown in Figs. 3.18 and 3.20, it is clearly observed that the modified Richardson plot of $ln(I_0/T^2)-q^2\sigma_0{}^2/2(kT)^2$ versus q/kT in Fig. 3.20 possesses a nearly linear characteristic after taking the barrier inhomogeneity phenomenon into consideration.

Comparing the linear approximation of the modified Richardson plot shown in Fig. 3.20 to Eq. (3.19), the value of the effective Richardson constant is determined as $A^* \sim 19.54 Acm^{-2}K^{-2}$ for the given diode area of A ~0.785×10^{-2} cm^{-2}. The results for the zero-bias mean barrier height and the Richardson constant are believed to the best for any ZnO thin film based Schottky diodes fabricated by thermal deposition method.

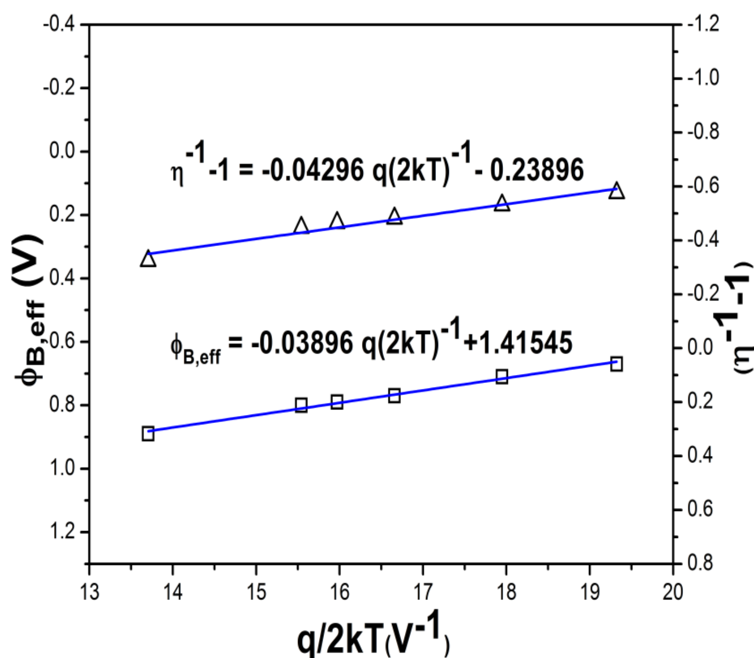

Figure 3.19: Typical $\phi_{B,eff}(T)$ versus $q/2kT$ and $\left(\eta^{-1}(T)-1\right)$ versus $q/2kT$ curves and their linear approximations by taking the effect of Gaussian distribution of barrier heights.

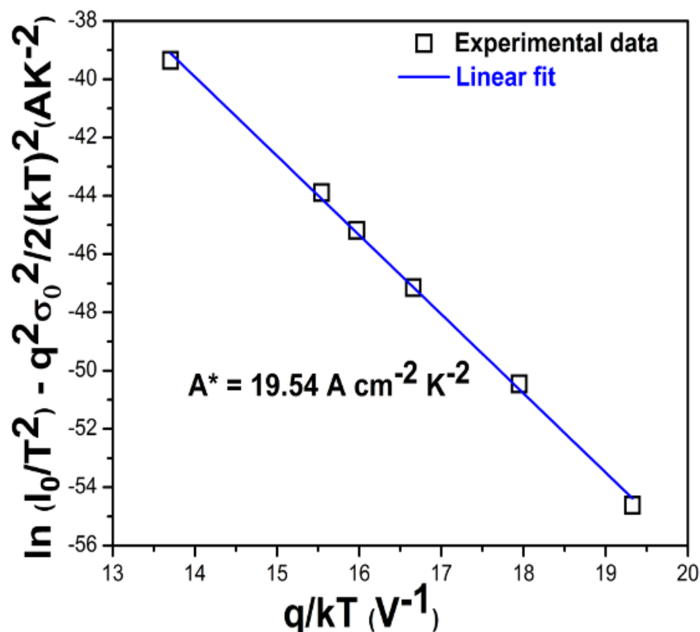

Figure 3.20: Plot of $ln\left(I_0/T^2\right)-q^2\sigma_0{}^2/2(kT)^2$ versus q/kT for determining the effective Richardson constant after taking the barrier inhomogeneity into consideration.

3.4. Summary and Conclusion

In the present chapter, we have fabricated Pd/ZnO thin film Schottky diodes on n-Si substrates by low cost thermal evaporation method. The surface morphology, chemical composition and crystalline structure of ZnO thin films have been determined by FESEM image, EDS spectrum and XRD spectrum respectively. The electrical chacterstics of Pd/ZnO thin film Schottky diodes have been investigated by room temperature I-V and C-V characteristics. Further, the temperature dependent I-V characteristics have been analyzed by taking Gaussian distribution of barrier heights into account. Some of the important observations from the present Chapter are given below:

- The as-grown ZnO thin films on n-Si substrates show nanocrystalline structure with hexagonal wurtzite phase of ZnO as confirmed by FESEM image and XRD pattern.
- The PL spectrum shows a strong near band edge (NBE) emission at wavelength of ~380 nm due to the excitonic transition between the valance band and conduction band.
- The value of different electrical parameters such as barrier height, ideality factor and series resistance have been calculated from room temperature I-V characteristics, Cheung's function and Norde's method
- The value of R_s (~30.983×10^3 Ω) obtained from the Norde's function is observed to be much higher than 5333 Ω and 4734 Ω estimated by using the conventional thermionic emission model and Cheung's approach respectively. The above large discrepancy in the value of R_s is attributed to non-suitability of the Norde's model for Schottky diodes with $\eta > 1$.
- The value of the barrier height is increased from 0.67 to 0.89 eV and value of ideality factor is decreased from 2.36 to 1.48 as the operating temperature is increased from 300 to 423K.
- The analysis of temperature-dependent I-V characteristics of Pd Schottky contacts on ZnO thin film grown on a n-Si<100> substrate by thermal evaporation method over a temperature range 300-423K provide the values of the zero-bias mean barrier height and effective Richardson constant as 1.41 eV and $19.54 Acm^{-2}K^{-2}$

respectively under the assumption of a Gaussian distributed barrier height across Pd/ZnO Schottky junction.

- The value of the zero-bias mean barrier height $q\phi_{B0,m}(T=0)=1.41\,eV$ is nearly equal to its theoretical value of 1.42 eV computed from the ideal Schottky-Mott theory by using the work function of Pd as 5.12 eV and electron affinity of ZnO as 3.7 eV.
- The estimated value of the effective Richardson constant is believed to be the first for Pd/ZnO thin film Schottky diodes. However, further improvement is required to obtain the Richardson constant closer to its theoretical value of $32\,Acm^{-2}K^{-2}$.